Title

Laser-Ablation Sampling for Accurate Analysis of Sulfur in Edible Salts

Journal

Applied Spectroscopy, 71(4)

ISSN

0003-7028

Authors

Lee, Yonghoon

Chirinos, Jose

Gonzalez, Jhanis

et al.

Publication Date

2017-04-01

DOI

10.1177/0003702817691288

Peer reviewed

Laser-Ablation Sampling for Accurate Analysis of Sulfur in Edible Salts

Yonghoon Lee,[1] Jose Chirinos,[2] Jhanis Gonzalez,[3,4] Dayana Oropeza,[3] Vassilia Zorba,[3] Xianglei Mao,[3] Jonghyun Yoo,[4] and Richard E. Russo[3,4]

[1]Department of Chemistry, Mokpo National University, Jeonnam 534-729, Republic of Korea

[2]Escuela de Química, Facultad de Ciencias, Universidad Central de Venezuela 1041a, Venezuela

[3]Lawrence Berkeley National Laboratory, Berkeley CA 94720, United States

[4]Applied Spectra, Inc., 46665 Fremont Boulevard, Fremont, CA 94538, United States

*Corresponding author: Richard E. Russo E-mail: rerusso@lbl.gov

Abstract

We evaluated the performance of laser-ablation analysis techniques such as LIBS, LA-ICP-OES and LA-ICP-MS, in comparison with that of ICP-OES using aqueous solutions for the quantification of sulfur in edible salts from different geographical origins. We found that the laser ablation based sampling techniques were not influenced by loss of sulfur, which was observed in ICP-OES with aqueous solutions for a certain salt upon their dissolution in aqueous solutions, originating from the formation of volatile species and precipitates upon their dilution in water. Although detection of sulfur using direct laser sampling with LA-ICP-MS has well-known isobaric and polyatomic interferences, LIBS and LA-ICP-OES showed good accuracy in the detection of sulfur for all salts. LIBS also provided the ability to identify the dominant chemical form in which sulfur is present in salts. Correlation between sulfur and oxygen, observed in LIBS spectra, provided chemical information about the presence of S^{2-} or SO_4^{2-}, which are associated with the origin and quality of edible salts.

Keywords Edible salt, Sulfur, Laser-Ablation Sampling, LIBS, LA-ICP-OES, ICP-OES

Introduction

Salt is a ubiquitously used food additive. Typically, a few to ten grams of salt is consumed by an average person per day.[1,2] According to the source from which salt is extracted, it can be generally classified into two categories; sea and rock salt.[3] Sea salt is produced by evaporating seawater on saltpans nearby sea shores whereas rock salts are collected from underground caverns. The as-extracted sea and rock salts (unrefined salts) are either refined for table salts or can be used for further processed salt products.

The elemental composition of salts depends on their sources and production methods. Sodium chloride (NaCl) is a common matrix for salts. Major metallic elements in salt are magnesium (Mg), calcium (Ca), and potassium (K), contained up to a few wt.%.[4–7] Minor metallic elements are strontium (Sr), lithium (Li), aluminum (Al), silicon (Si), titanium (Ti), and iron (Fe).[4,6,8–9] Their concentrations are typically less than a few hundred parts-per-million (ppm). Sulfur (S), oxygen (O), hydrogen (H), and carbon (C) are major non-metallic elements in salts. Most of S and O in salts come from sulfates (SO_4^{2-}) that were originally dissolved in seawater.[10] SO_4^{2-} is typically the most abundant ion in sea salts excluding the matrix ions, Cl^- and Na^+. O also may be included in forms of carbonates (CO_3^{2-}), bicarbonates (HCO_3^-), other oxyanions and water (H_2O) that was absorbed by hygroscopic compounds in salts such as $MgSO_4$ and $MgCl_2$.[7,11]

Chemical analysis of edible salts is necessary for evaluating their quality, distinguishing their geographical origin or production method, and monitoring toxic chemical species. To date, the majority of the studies on quantitative analysis of salts have used inductively coupled plasma optical emission spectroscopy (ICP-OES) and atomic absorption spectroscopy (AAS).[4,5,12–14] Other techniques used for quantitative analysis of salt are ICP-MS,[15] instrumental neutron activation analysis (INAA),[16–19] combination of chromatography and spectrophotometry,[8,20–22] and gas chromatography-mass spectrometry (GC-MS).[25] Fourier-transform near-infrared (FT-NIR) spectroscopy[5], LIBS,[6,7,9,23] and combination of laser-

ablation inductively coupled plasma mass spectroscopy (LA-ICP-MS) and LIBS[24] have been use for classification of salts.

Among the various elements contained in edible salts, analysis of S is particularly important. S is an essential nutritional element involved in forming important amino acids such as methionine and cysteine which play an important role in maintaining and supporting human immune function.[26] In most unrefined salts, S is contained in the form of SO_4^{2-}. However, some particular salts, such as the Himalayan black salt produced in India and the Korean bamboo salt, contain S in the form of sulfide (S^{2-}), not SO_4^{2-}. These salts are widely marketed for their health benefits. For example, the presence of S^{2-} in bamboo salt was identified as a potential agent to cure allergic inflammation.[29] Therefore, accurate analysis of S in various types of edible salts is important for their quality evaluation and also useful for selecting better raw unrefined salts for processed products.

In this work, we compare laser-ablation sampling for accurate analysis of S in edible salts over conventional aqueous solution ICP-OES analysis. LA-ICP-OES, LIBS and LA-ICP-MS analyses were performed on solid pellets of edible salts from different geographical origins. We found that laser-ablation sampling offered more accurate comparison of the total amount of S among various edible salts over aqueous ICP-OES. This was because laser ablation sampling does not suffer from loss of sulfur which occurs for the aqueous solutions of certain types of salts, due to vaporization in the form of hydrogen sulfide (H_2S) or precipitation as insoluble metal sulfides during preparation of the aqueous solution samples. The intensity correlations of the S I and with O I lines observed in LIBS spectra indicate that the rock salt contains a relatively large amount of S in a different chemical form (S^{2-}) than that of the other salts, i.e. SO_4^{2-}. To the best of our knowledge, S in edible salts has been analyzed by turbidimetry assuming that S exists in form of SO_4^{2-}. In this analysis, barium chloride ($BaCl_2$) is added to aqueous solution of edible salts and makes insoluble particles of barium sulfate ($BaSO_4$) that scatter light.[4,15] This method would provide inaccurate results for salt samples containing relatively large amounts of S^{2-}. ICP-OES, ICP-MS, and AAS have been used to analyze metallic elements in edible

77 salts.[4,5,12–14] For preparing the sample solutions, deionized water or nitric acid solution were used. As we
78 observed, water has the loss problem for S when it is in the S^{2-} form. Moreover, in a nitric acid solution,
79 insoluble metal sulfides can be decomposed more easily to soluble metal nitrate and gaseous H_2S that
80 leads to S loss. Laser-ablation sampling requires no solvents and no chemicals such as acids for
81 digesting insoluble matters. This strength of laser-ablation sampling enables us to use a single
82 spectroscopic analysis technique for most of the important elements (including S) contained in edible
83 salts. Also, our results underscore LIBS as a promising technique for rapid accurate analysis of S in
84 edible salts and indirect establishment of its speciation in salts.
85
86 **Experimental**
87 *Salt samples and ICP-OES analysis of aqueous solution samples*
88 Eight commercially available edible salts of different origin were collected for this work. Three of them
89 are sea salts and the others are rock salts. The geographical origins and types of the salt samples are
90 listed in Table 1 along with the sample code, which will be used from this point as sample identifiers.
91 The S concentrations determined by ICP-OES using aqueous solutions of the sample salts are also listed
92 in Table 1. For the ICP-OES analysis, standard solutions were prepared by dissolving and diluting
93 mixtures of NaCl (≥99.0 %, VWR, Radnor, Pennsylvania, USA) and $MgSO_4$ (≥99.5%, Sigma-Aldrich,
94 St. Louis, MO) powders in distilled water. The mixtures of NaCl and $MgSO_4$ with S concentrations from
95 0 to 3.72 wt.% were dissolved in distilled water by a dilution factor of 1/5000. The S I line intensity at
96 182.034 nm was measured for the standard solutions by an ICP-OES spectrometer (5100 ICP-OES,
97 Agilent Technologies). A power of 1300 W was applied for plasma generation. Argon gas was used for
98 coolant, auxiliary, and nebulizer (cross) flows with flow rates of 12, 1.0, and 0.7 L/min, respectively.
99 The uptake rate of the aqueous solutions was 1.0 mL/min. Figure 1 shows the calibration curve for S
100 obtained by ICP-OES. With a dilution factor of 1/5000, we obtained a good linear correlation of
101 intensity versus concentrations for the whole concentration range studied. Similarly, for the sample salts,

their powders were also dissolved and diluted in distilled water by a factor of 1/5000 before measuring the S I line intensity under the same conditions.

LA-ICP-OES

For LA-ICP-OES analysis, the salt samples were milled and homogenized into a fine powder using a ball mill (8000M Mixer/Mill®, SPEX Sample Prep). Five grams of each salt was put in an agate vial with an agate ball and then rotated at 1450 rpm for 10 min. A 0.5 g of the milled powder was pelletized into a 13-mm diameter disc using an automated press (3630 X-PRESS®, SPEX Sample Prep) under 7 ton pressure for 10 min. The same ICP-OES spectrometer that was used for the analysis of aqueous solution samples was employed for the analysis of solid sample pellets; the nebulizer and spray chamber were exchanged with a laser-ablation instrument (J200 LA Instrument, Applied Spectra, Inc.). A Q-switched Nd:YAG laser beam was focused on the surface of the pellet sample (5× magnification, 35 mm working distance) placed in the laser-ablation chamber. The wavelength, pulse duration, pulse energy, repetition rate and spot size on the sample surface were 213 nm, 10 ns, 5 mJ/pulse, 10 Hz, and 150 μm in diameter, respectively. For each sample pellet, a 2-mm length line scan composed of 200 laser shots was performed five times. Helium was used to transport ablated particles to the ICP-OES spectrometer. A power of 1500 W was applied for plasma generation. Argon gas was used for coolant, auxiliary, and nebulizer (cross) flows with flow rates of 18, 1.8, and 1.0 L/min, respectively.

LIBS

For LIBS analysis, sample pellets were prepared using the same process as for the LA-ICP-OES analysis. The LIBS spectra of the ten salt pellet samples were obtained using a commercial instrument (J200 LIBS Instrument, Applied Spectra, Inc.). The sample pellet was enclosed in a sampling chamber. A Q-switched Nd:YAG laser beam was focused on the surface of salt pellets by an objective lens (5× magnification, 35 mm working distance) through a quartz window. The wavelength, pulse duration,

pulse energy, repetition rate, and spot size in diameter on the sample surface were 266 nm, 10 ns, 20 mJ/pulse, 10 Hz, and 150 μm, respectively. For sulfur analysis using LIBS, three spectral regions are generally considered; (i) vacuum ultraviolet,[30,31] (ii) visible,[31,32] and (iii) near-infrared spectral regions.[31,33–35] Herein, the near-infrared region, where the three S I lines are located at 921.287, 922.809, and 923.754 nm, was selected. Helium ambient gas was used to enhance the S I line intensity.[33,34] The optical emission from the laser-induced plasma was collected by a lens doublet through the sample chamber top quartz window and sent to a 6-channel charge-coupled device (CCD) spectrometer with ~0.1 nm spectral resolution and wavelength coverage between 190 and 1040 nm through an optical fiber bundle. The CCD detection gate width was 1.05 ms and delayed from the laser pulse by 500 ns to optimize the signal-to-background ratio. For each sample, a 110-mm raster scan composed of 5600 laser shots was performed on the pellet surface. The 5600 single-shot LIBS spectra were divided into 5 groups sequentially and accumulated to 5 spectra to be analyzed.

LA-ICP-MS

For LA-ICP-MS analysis, pellet samples were prepared in the same process as for the LA-ICP-OES analysis. A Q-switched Nd:YAG laser beam was focused on the sample surface by an objective lens (5× magnification, 35 mm working distance). The wavelength, pulse duration, pulse energy, repetition rate, and spot size on the sample surface were 213 nm, 10 ns, 5 mJ/pulse, 10 Hz, and 150 μm in diameter, respectively. The particles ablated in the laser-ablation sampling system were transported to a quadrupole mass spectrometer (Plasma Quant MS Elite, Analytik Jena) by using helium as a carrier gas flowing at a rate of 0.3 L/min. The forward power was set to 1400 W with 18.0 L/min Ar gas, auxiliary flow rate of 18 L/min, and sheath gas flow rates of 0.8 L/min. The mass spectra were recorded in the region of $m/z = 31.5 - 35.5$.

Results and Discussion

Calibration curves of LA-ICP-OES and LIBS

Figure 2 shows the calibration curves for S acquired by LA-ICP-OES (a) and LIBS (b), and the LIBS spectra of eight salt samples in the wavelength region between 918 and 932 nm (c). In the LA-ICP-OES analysis, the intensities of the two emission lines, S I and Cl I lines at 181.972 and 774.497 nm, respectively, were measured. The intensity ratio of the S I line to the Cl I line was used for the calibration curve. In the near-infrared wavelength region of the LIBS spectra, three strong S I lines were observed at 921.287, 922.809, and 923.754 nm along with Cl I, Mg II, and O I lines as shown in Figure 2c.[36] In the case of LIBS, the intensity normalization, i.e. the ratio of the S I line intensity to the Cl I line intensity, did not improve significantly the linearity of the calibration curve or analysis precision as much as it did in the case of LA-ICP-OES. However, the direct use of the S I line intensity was enough to obtain a linear calibration curve. For the LIBS calibration curve, the peak areas at 922.809 and 923.754 nm were integrated and their sum was used for the calibration. As can be seen in Figure 2c, the strongest S I line at 921.287 nm partially overlaps the nearby Mg II line at 921.825 nm and was therefore excluded. As was mentioned in the experimental section, the true S concentrations in the salt samples were assumed to be that measured from the ICP-OES analysis of the aqueous solutions of salts. In both the analyses of LA-ICP-OES and LIBS, the seven salt samples excluding the HI sample show strong positive correlations of their signal intensities with the concentrations of S, and provide linear calibration curves in the 0.15 to 1.3 wt.%, range (R^2 values: 0.9964 for LA-ICP-OES and 0.9987 for LIBS). However, the S I lines chosen for LIBS analysis result from the emission between high-lying excited levels with the lower-level energy of 52623.64 cm^{-1} so as to minimize self-absorption. The spectroscopic parameters of these S I lines are listed in Table 2. The limits of detection (LODs) for S were estimated for the LA-ICP-OES and LIBS analyses using the following equation.

$$\mathrm{LOD} = \frac{3\sigma}{s} \quad (1)$$

For each analysis, σ is the standard deviation from five measurements for the salt sample from Poland (PL) that contains the least amount of S. *s* is the slope of each calibration curve. The LODs for S were 0.074 wt.% for LA-ICP-OES, and 0.12 wt.% for LIBS analysis.

The HI sample consistently shows a deviation from linearity in the calibration curves of LA-ICP-OES and LIBS in Figures 2a and 2b, respectively. In contrast to these correlations, the LA-ICP-OES and LIBS signals (Figure 3) show a linear relationship (R^2 = 0.9935 of the linear fit) and also strong positive correlation (Pearson's correlation coefficient $\rho = 0.9972$), including the HI sample,

LA-ICP-MS analysis of ^{34}S

In order to understand the deviation of certain samples from linearity in the calibration curves (Figures 2a and 2b), another laser ablation sampling technique, LA-ICP-MS, was used for the five salt samples (JD, HI, HJ, HP, and MG) to compare and correlate the S mass signal to the results obtained by LIBS with solid pellets and ICP-OES with aqueous solutions. S is one of the difficult elements to analyze with ICP-MS due to well-known isobaric and polyatomic interferences.[37,38] S has four stable isotopes, ^{32}S (95.02%), ^{33}S (0.75%), ^{34}S (4.21%), and ^{36}S (0.02%).[39] Among these, ^{34}S was chosen for this analysis, to avoid the interference of $^{32}S^+$ with $^{16}O_2^+$. A background spectrum was recorded without firing the ablation laser and was subsequently subtracted from the LA-ICP-MS spectrum of each salt sample. The LA-ICP-MS spectrum of the HI sample and the corresponding background spectrum are provided in the Supplemental material (Figure S1). To confirm that the mass peak intensity at m/z = 34 originated from ^{34}S, and not molecules or other isobaric isotopes, the mass peak intensity ratios of $^{34}S/^{33}S$ for the salt samples were compared with the corresponding natural abundance ratio (5.61) (see Figure S2 in the Supplemental material).

In Figure 4a, the ^{34}S isotope signal intensities are plotted versus the S concentration determined by the ICP-OES analysis for the aqueous solutions. The poor precision of the LA-ICP-MS analysis is mainly due to the weak mass signal intensity of ^{34}S. However, similarly to the LA-ICP-OES and LIBS

analyses, LA-ICP-MS provided a linear calibration with the exception of the HI sample. However, the ^{34}S mass signal intensity showed a linear relation with the S I line intensity of LIBS including the HI sample (see Figure 4b). The same was observed for LA-ICP-OES and LA-ICP-MS signal intensities. This LA-ICP-MS analysis result confirmed that the S concentration in the HI sample was greater than that determined by the ICP-OES analysis for its aqueous solution.

S loss mechanism

The S concentration of the HI sample calculated from the LA-ICP-OES (Figure 2a), LIBS (Figure 2b), and LA-ICP-MS (Figure 4a) calibration curves are plotted in Figure 5, along with the S concentration directly measured from the aqueous ICP-OES analysis. The concentrations calculated from the laser-ablation sampling techniques, agree well with one another within their 1σ error bars (LA-ICP-OES: 0.804 ± 0.093 wt.% , LIBS: 0.823 ± 0.068 wt.%, LA-ICP-MS:, 0.76 ± 0.17 wt.%). These concentrations are consistently greater than that resulting from the aqueous ICP-OES analysis of the HI sample (0.470 ± 0.010 wt.%).

The dissolution of the HI sample in water to prepare its aqueous solution for ICP-OES analysis generated both a very strong odor associated with the presence of H_2S and a relatively large amount of insoluble precipitates. The most common sulfur species in most edible salts, SO_4^{2-}, is not prone to vaporization and precipitation when dissolved in water. Although clear identification of the chemical forms of S^{2-} in the HI sample, based on instrumental analyses, has not been reported so far, the significant amount of S^{2-} may exist in the forms of sulfides of Na, K, Mg, and Ca that are abundant in edible salts. MgS and CaS decompose into their hydroxides and generate H_2S in water. Na_2S primarily produces bisulfide ion (HS^-) in its aqueous solution, but generates H_2S even in contact with moist air following the reaction of $Na_2S + H_2O + CO_2 \rightarrow Na_2CO_3 + H_2S$.[40] All of the sulfides, Na_2S, K_2S, MgS, and CaS make the aqueous solution basic. The alkaline nature of the HI aqueous solution was verified (see the images of pH papers in Figure S3 of the Supplementary material) supporting the presence of

these alkali or alkaline earth metal sulfides. Also, the insolubility of transition metal sulfides such as iron sulfide can be suggested as the other possible S loss mechanism through precipitation. Of the 3.343 g of HI sample dissolved in distilled water, 0.031 g of insoluble particles were filtered and collected, amounting to a percentage of 0.92 wt.%.

The intensity correlation between the S I and O I LIBS lines in Figure 6 provides a means discriminating between chemical forms of S in the salt samples. To obtain the intensity values, baseline-subtracted integrated peak areas were taken for the three overlapping O I lines at 777.194, 777.417, and 777.539 nm, and the two S I lines at 922.809 and 923.754 nm. The LIBS spectra for O I lines are shown as the inset of Figure 6. All salts, excluding the HI sample, form a trend of positive correlation between the S I and O I line intensities. This observation is consistent with SO_4^{2-} as the most prevalent form of S in most edible salts. For the HI sample, the O I intensity is relatively low as compared to the rest of the salts with similar S I emission intensity, and again is consistent with the presence of S^{2-} rather than SO_4^{2-}.

Finally, the following three facts exclude the possibility of strong matrix effects enhancing the S I line intensity particularly for the LIBS spectrum of the HI sample:

(i) Our samples have a common matrix, NaCl.

(ii) The optical emission spectroscopic techniques (LIBS and LA-ICP-OES) and the mass spectrometry (LA-ICP-MS) showed consistent results. This indicates that the S I line intensity in the LIBS spectra reflect the mass of S ablated from the samples and the S I line intensity of the HI sample was not enhanced by any matrix effects further heating the laser-induced plasma.

(iii) A plot of the Mg I line intensity observed in the LIBS spectra versus the Mg concentrations obtained from the aqueous-solution ICP-OES analysis shows no significant deviation for the HI sample. This excludes the possibility of a particularly large amount of ablated mass for the HI sample (see Figure S4 in the Supplementary material).

Conclusions

Three laser ablation sampling techniques, LA-ICP-OES, LIBS and LA-ICP-MS were used for the analysis of S in edible salts from different geographical origin. These techniques provided reliable calibrations to the concentrations of S determined by ICP-OES using aqueous solution samples. However, for the Himalayan rock salt from India, all laser ablation sampling techniques measured a concentration significantly higher than the corresponding values predicted by ICP-OES for the aqueous solution samples. This effect was traced to ample loss of sulfur in the rock salt when it was dissolved in water for ICP-OES analysis through vaporizing as H_2S or precipitating as insoluble metal sulfides. For these samples, all laser ablation techniques provided good results for accuracy and sensitivity. In addition, LIBS stands out for the analysis of S in salts due to its simplicity and ability to provide information about speciation. The intensity correlations of the S I and O I LIBS lines indicate that the rock salt contains relatively large amount of S in a different chemical form (S^{2-}) from that of the other salt samples (SO_4^{2-}).

Conflict of Interest

The authors report there are no conflicts of interest.

Funding

This paper was supported by Research Funds of Mokpo National University in 2015. The research at the Lawrence Berkeley National Laboratory was supported by the Office of Basic Energy Sciences, Chemical Science Division of the U.S. Department of Energy under contract number DE-AC02-05CH11231.

Supplemental Material

All supplemental material mentioned in the text, which includes three figures, is available in the online version of the journal, at http://s-a-s.org.

References

[1] M.J. Morris, E.S. Na, A.K. Johnson. “Salt Craving: The Physiology of Pathogenic Sodium Intake”. Physiol. Behav. 2008. 94(5): 709–721.

[2] M. O’Donnell, M.J. McQueen, H. Yan, A. Rosengren, A. Averzum, R. Iqbal, S. Gulec, R. Yusuf, G. Dagenais, S. Yusuf. “Urinary Sodium and Potassium Excretion, Mortality, and Cardiovascular Events”. New Engl. J. Med. 2014. 371(7): 612–623.

[3] Salt Institute. “Production & Industry”. http://saltinstitute.org/salt-101/production-industry/ [accessed April 11 2016].

[4] S.L. Drake, M.A. Drake. “Comparison of Salty Taste and Time Intensity of Sea and Land Salts from around the World”. J. Sensory Studies. 2011. 26(1): 25–34.

[5] A.C. Galvis-Sánchez, J.A. Lopes, I. Delgadillo, A.O.S.S. Rangel. “Fourier Transform Near-Infrared Spectroscopy Application for Sea Salt Quality Evaluation”. J. Agric. Food Chem. 2011. 59(20): 11109–11116.

[6] M.M. Tan, S. Cui, J. Yoo, S.-H. Han, K.-S. Ham, S.-H. Nam, Y. Lee. “Feasibility of Laser-Induced Breakdown Spectroscopy (LIBS) for Classification of Sea Salts”. Appl. Spectrosc. 2012. 66(3): 262–271.

[7] G. Park, H. Yoo, Y. Gong, S. Cui, S.-H. Nam, K.-S. Ham, J. Yoo, S.-H. Han, Y. Lee. “Feasibility of Rapid Classification of Edible Salts by a Compact Low-Cost Laser-Induced Breakdown Spectroscopy Device”. Bull. Kor. Chem. Soc. 2015. 36(1): 189–197.

[8] Y. Akama, A. Tong. “High-Performance Liquid Chromatographic Determination of Aluminum and Iron(III) in Solar Salt in the Form of Their 1-Phenyl-3-Methyl-4-Benzoyl-5-Pyrazolone Chelates”. J. Chromatogr. A. 1993. 633(1–2): 129–133.

297 [9] Y. Lee, K.-S. Ham, S.-H. Han, J. Yoo, S. Jeong. “Revealing Discriminating Power of the Elements
298 in Edible Sea Salts: Line-Intensity Correlation Analysis from Laser-Induced Plasma Emission Spectra”.
299 Spectrochim. Acta Part B. 2014. 101: 57–67.

300 [10] A.C. Galvis-Sánchez, J.A. Lopes, I. Delgadillo, A.O.S.S. Rangel. “Sea Salt”. In: M. de la Guardia,
301 A. Conzálvez, editors. “Food Protected Designation of Origin Methodologies and Applications”.
302 Comprehensive Analytical Chemistry. 2013. 60: 719–740.

303 [11] M.J. Atkinson, C. Bingman. “Elemental Composition of Commercial Sea Salts”. J. Aquatic. Aquat.
304 Sci. 1997. 8(2): 39–43.

305 [12] M. Soylak, D.S.K. Peker, O. Turkoglu. “Heavy Metal Contents of Refined and Unrefined Table
306 Salts from Turkey, Egypt and Greece”. Environ. Monit. Assess. 2008. 143(1–3): 267–272.

307 [13] H. Pourgheysari, M. Moazeni, A. Ebrahimi. “Heavy Metal Content in Edible Salts in Isfahan and
308 Estimation of Their Daily Intake via Salt Consumption”. Int. J. Env. Health Eng. 2012. 1(1): 41–45.

309 [14] M.A. Herrador, A.G. González, A.G. Asuero. “Inorganic Indicators of the Origin of Edible Salts
310 Marketed in Spain from a Chemometric Approach”. J. Food Prot. 1998. 61(7): 891–895.

311 [15] S. Ji, T. Yabutani, A. Itoh, K. Chiba, H. Haraguchi. “Distributions of Elements into Natural Salt
312 from Coastal Seawater in a Natural-Salt Preparation Process”. Bunseki Kagaku. 2000. 49(2): 111–119.

313 [16] G. Steinhauser, J.H. Sterba, K. Poljanc, M. Bichler, K. Buchtela. “Trace Elements in Rock salt and
314 Their Bioavailability Estimated from Solubility in Acid”. J. Trace Elem. Med. Biol. 2006. 20(3): 143–
315 153.

316 [17] M. Yui, Y. Kikawada, T. Oi, T. Honda, D. Sun, K. Shuai. “A Preliminary Investigation on the
317 Determination of Lanthanoids, Thorium and Uranium in Brine and Deposit of a Salt Lake in China”. J.
318 Radioanal. Nucl. Chem. 1997. 231(1–2): 83–86.

[18] M. Yui, Y. Kikawada, T. Oi, T. Honda, T. Nozaki. “Abundance of Lanthanoids in Rock Salts Determined by Neutron Activation Analysis”. J. Radioanal. Nucl. Chem. 1998. 238(1–2): 3–6.

[19] M. Yui, Y. Kikawada, T. Oi, T. Honda, T. Nozaki. “Abundance of Uranium and Thorium in Rock Salts”. Radioisotopes. 1998. 47(6): 488–492.

[20] T. Yamane, H. Yamada. “Flow-Injection Spectrophotometric Determination of Trace Iron in Various Salts, Elimination of Blank Peak Effect and Use of 2-(5-Nito-2-Pyridylazo)-5-(N-Propyl-N-Sulfopropylamino) Phenol as Chromogenic Agent”. Anal. Chim. Acta. 1995. 308(1–3): 433–438.

[21] T. Yamane, K. Koshino. “Flow-Injection Systems for Determination of Trace Manganese in Various Salts by Catalytic Photometric Detection”. Talanta. 1996. 43(6): 963–969.

[22] V.V. Kuznetsov, Y.V. Ermolenko, L. Seffar. “Amylose and Amilopectin as Reagents for the Flow-Injection Determination of Elemental Iodine”. J. Anal. Chem. 2007. 62(5): 479–485.

[23] V.K. Singh, N.K. Rai, S. Pandhija, A.K. Rai, P.K. Rai. “Investigation of Common Indian Edible Salts Suitable for Kidney Disease by Laser Induced Breakdown Spectroscopy”. Lasers Med. Sci. 2009. 24(6): 917−924.

[24] Y. Lee, S.-H. Nam, K.-S. Ham, J. Gonzalez, D. Oropeza, D. Quarles Jr., J. Yoo, R.E. Russo. “Multivariate Classification of Edible Salts: Simultaneous Laser-Induced Breakdown Spectroscopy and Laser-Ablation Inductively Coupled Plasma Mass Spectrometry Analysis”. Spectrochim. Acta Part B. 2016. 118: 102–111.

[25] I. Silva, S.M. Rocha, M.A. Coimbra. “Headspace Solid Phase Microextraction and Gas Chromatography-Quadrupole Mass Spectrometry Methodology for Analysis of Volatile Compounds of Marine Salt as Potential Origin Biomarkers”. Anal. Chim. Acta. 2009. 635(2): 167–174.

340 [26] R.F. Grimble. “The Effects of Sulfur Amino Acid Intake on Immune Function in Humans”. J. Nutri.
341 2006. 136(6): 1660S–1665S.

342 [27] F. Case. 1001 Foods You Must Taste Before You Die. New York, NY: Universe Publishing, 2008.
343 Pp.676.

344 [28] L. Moorjani. Ajanta: Regional feast of India. Layton, UT: Gibbs Smith, 2005. Pp. 22.

345 [29] N.-R. Han, P.D. Moon, H.-J. Jeong, H.-M. Kim. “Hydrogen Sulfide Diminishes the Levels of
346 Thymic Stromal Lymphopoietin in Activated Mast Cells”. Arch. Dermatol. Res. 2016. 308(2): 103–113.

347 [30] X. Jiang, P. Hayden, J.T. Costello, E.T. Kennedy. “Double-Pulse Laser Induced Breakdown
348 Spectroscopy with Ambient Gas in the Vacuum Ultraviolet: Optimization of Parameters for Detection
349 of Carbon and Sulfur in Steel”. Spectrochim. Acta Part B. 2014. 101: 106–113.

350 [31] M. Gaft, L. Nagli, I. Fasaki, M. Kompitsas, G. Wilsch. “Laser-Induced Breakdown Spectroscopy
351 for On-Line Sulfur Analyses of Minerals in Ambient Conditions”. Spectrochim. Acta Part B. 2009.
352 64(10): 1098–1104.

353 [32] M.A. Gondal, A. Dastageer, M. Maslehuddin, A.J. Alnehmi, O.S.B. Al-Amoudi. “Detection of
354 Sulfur in the Reinforced Concrete Structures Using a Dual-Pulsed LIBS System”. Opt. Laser Technol.
355 2012. 44(3): 566–571.

356 [33] F. Weritz, D. Schaurich, G. Wilsch. “Detector Comparison for Sulfur and Chlorine Detection with
357 Laser Induced Breakdown Spectroscopy in the Near-Infrared Region”. Spectrochim. Acta Part B. 2007.
358 62(12): 1504–1511.

359 [34] F. Weritz, S. Ryahi, D. Schaurich, A. Taffe, G. Wilsch. “Quantitative Determination of Sulfur
360 Content in Concrete with Laser-Induced Breakdown Spectroscopy”. Spectrochim. Acta Part B. 2005.
361 60(7–8): 1121–1131.

362 [35] T.A. Labutin, A.M. Popov, S.M. Zaytsev, N.B. Zorov, M.V. Belkov, V.V. Kiris, S.N. Raikov.
363 "Determination of Chlorine, Sulfur and Carbon in Reinforced Concrete Structures by Double-Pulse
364 Laser-Induced Breakdown Spectroscopy". Spectrochim. Acta Part B. 2014. 99: 94−100.

365 [36] The National Institute of Standards and Technology (NIST). "NIST Atomic Spectra Database".
366 2012. http://www.nist.gov/pml/data/asd.cfm. [accessed April 11 2016].

367 [37] S.H. Tan, G. Horlick. "Background Spectral Features in Inductively Coupled Plasma/Mass
368 Spectrometry". Appl. Spectrosc. 1986. 40(4): 445–460.

369 [38] E. Albalat, P. Telouk, V. Balter, T. Fujii, V.P. Bondanese, M.-L. Plissonnier, V. Vlaeminck-
370 Guillem, J. Baccheta, N. Thiam, P. Miossec, F. Zoulim, A. Puisieuxg, F. Albarède. "Sulfur Isotope
371 Analysis by MC-ICP-MS and Application to Small Medical Samples". J. Anal. At. Spectrom. 2016.
372 31(4): 1002–1011.

373 [39] D.R. Lide. Handbook of Chemistry and Physics. Boca Raton, FL: CRC Press, Inc., 1994. Pp. 1-10.

374 [40] P. Patnaik. Handbook of Inorganic Chemicals. New York, NY: McGraw-Hill Companies, Inc.,
375 2002. Pp. 880.

Table 1. Sample list and S concentrations analyzed by ICP-OES for aqueous solution samples.

Sample code	Geographical origin	Type	S conc. (mg/Kg)
HJ	Hokkaido Japan	Sea salt	4700 ± 100
HI	Himalaya, India	Rock salt	5750 ± 120
HP	Himalaya, Pakistan	Rock salt	3259 ± 70
JD	Jeung-Do, South Korea	Sea salt	9200 ± 200
MAB	Mt. Andes, Bolivia	Rock salt	1811 ± 39
MG	Mongolia	Rock salt	1900 ± 41
OJ	Okinawa, Japan	Sea salt	13098 ± 290
PL	Poland	Rock salt	1549 ± 32

Table 2. Spectroscopic parameters of S I lines observed in LIBS spectra.

Observed wavelength (nm)	Transition probability (s^{-1})	Lower-level energy (cm^{-1})	Upper-level energy (cm^{-1})	Lower-level statistical weight	Upper-level statistical weight
912.287	2.79×10^{7}	52623.640	63475.051	5	7
922.809	2.77×10^{7}	52623.640	63457.142	5	5
923.754	2.77×10^{7}	52623.640	63446.065	5	3

Figure 1. Calibration curve of S obtained by ICP-OES analysis for standard solutions of NaCl-$MgSO_4$ mixtures.

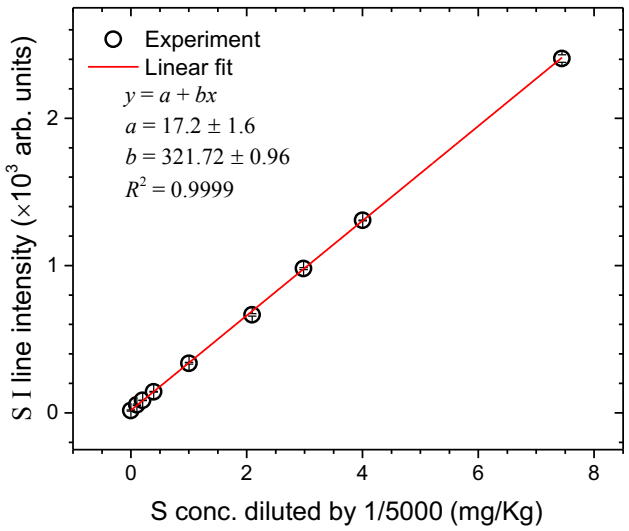

Figure 2. Calibration curves of S developed by LA-ICP-OES (a) and LIBS (b), and the LIBS spectra of eight salt samples in the wavelength region between 918 and 932 nm (c).

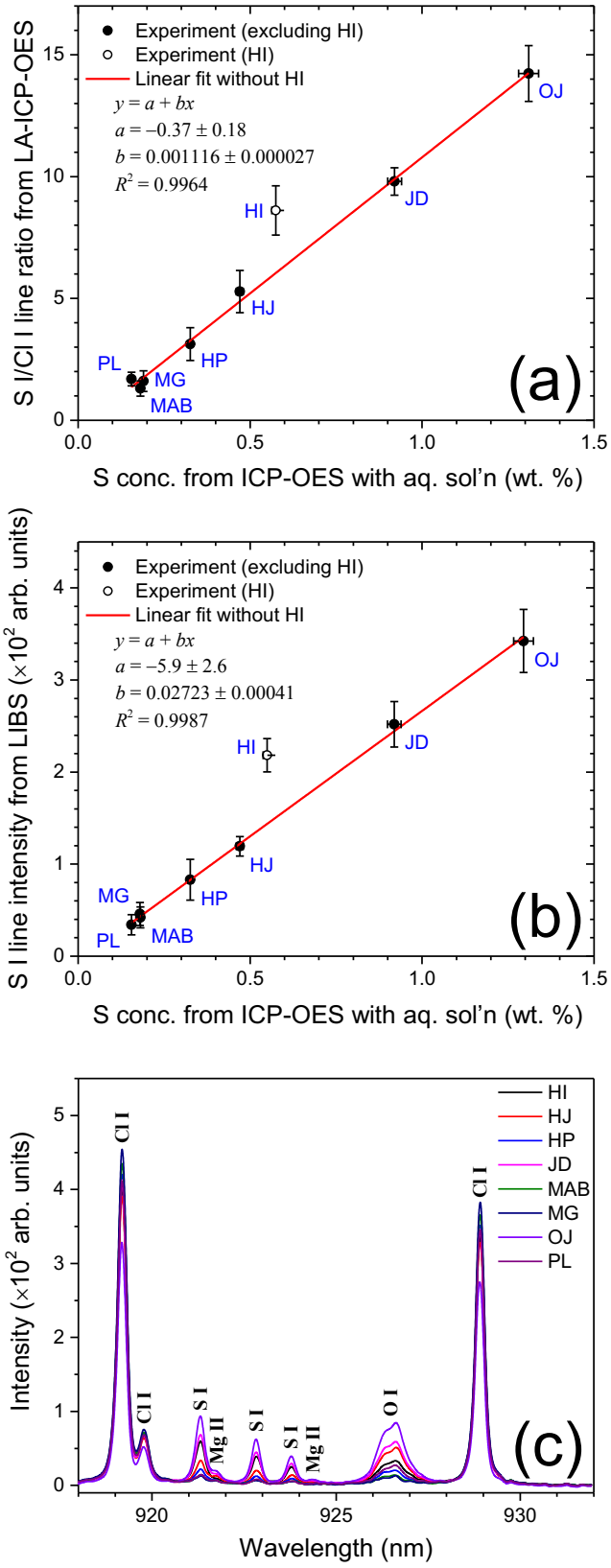

Figure 3. The plot of the signal intensities from LIBS with respect to those from LA-ICP-OES.

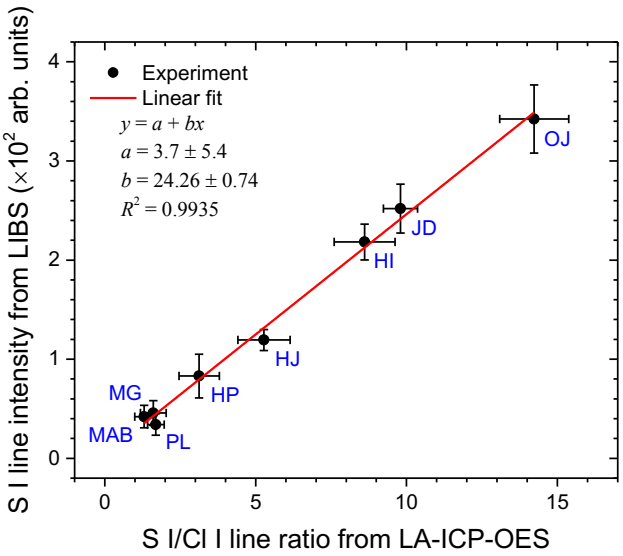

Figure 4. Plots of ^{34}S isotope signal intensities with respect to the S concentrations determined by the ICP-OES analysis for aqueous solution samples (a) and the S I line intensities observe in LIBS spectra (b).

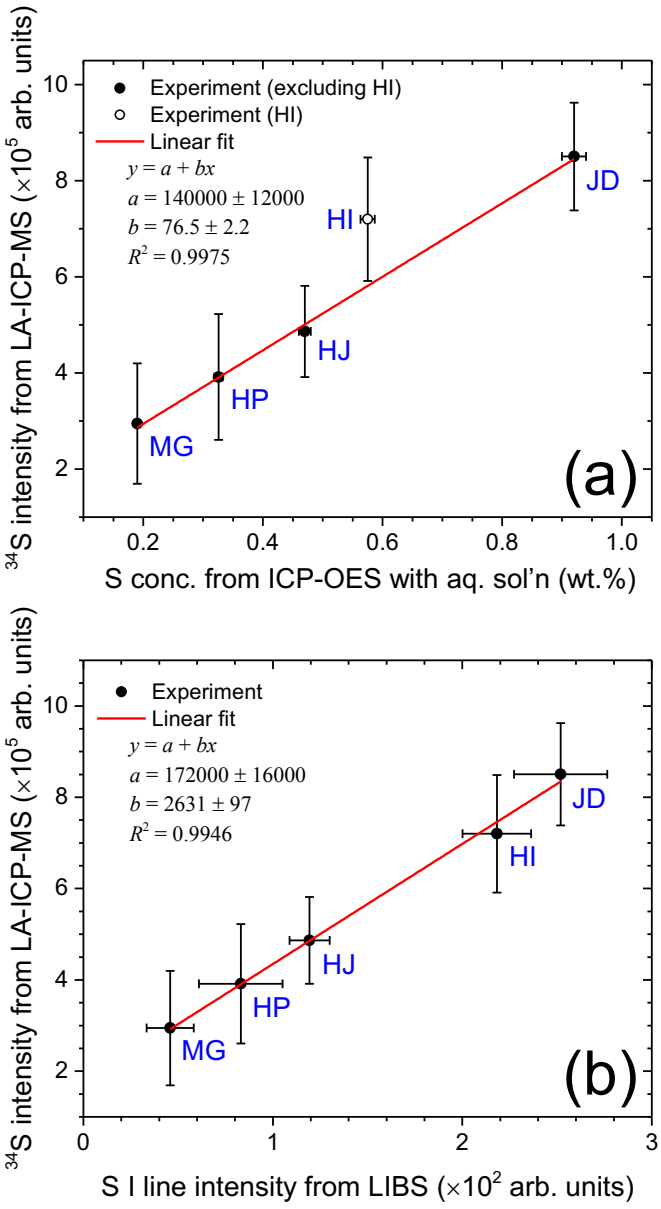

Figure 5. S concentrations in the HI sample estimated by LA-ICP-OES, LIBS, LA-ICP-MS, and ICP-OES analysis for the aqueous solution samples.

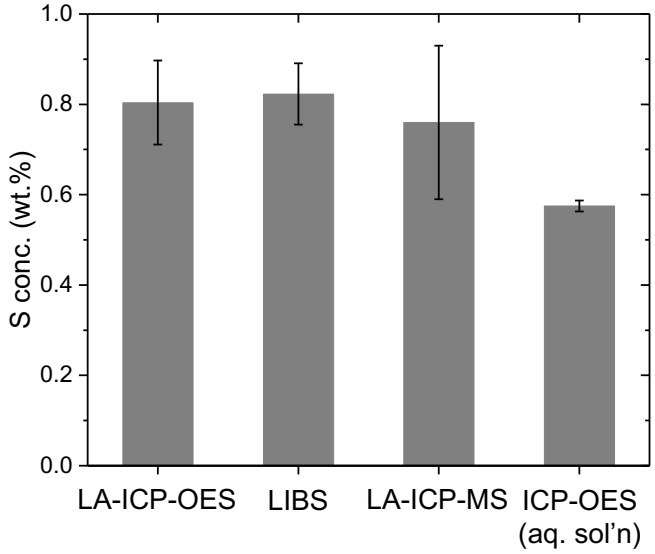

Figure 6. Plot of the O I line intensities observed in the LIBS spectra of the eight salt samples with respect to the corresponding S I line intensities.